Chemical Engineering Journal 426 (2021) 131282

Contents lists available at ScienceDirect

Chemical Engineering Journal

journal homepage: www.elsevier.com/locate/cej

A hybrid molecular sensitizer for triplet fusion upconversion

Xinyu Wang [a], Xing Wang [b], Glib V. Baryshnikov [f,h], Rashid R. Valiev [g,h], Rongwei Fan [b], Songtao Lu [a], Hans Ågren [a,e,i], Guanying Chen [a,c,d,*]

[a] School of Chemistry and Chemical Engineering, Harbin Institute of Technology, Harbin 150090, China
[b] School of Astronautics, Harbin Institute of Technology, Harbin 150001, China
[c] Key Laboratory of Micro-systems and Micro-structures, Ministry of Education, Harbin Institute of Technology, Harbin 150001, China
[d] State Key Laboratory of Urban Water Resource and Environment, Harbin Institute of Technology, Harbin 150001, China
[e] Department of Physics and Astronomy, Uppsala University, Uppsala, Sweden
[f] Laboratory of Organic Electronics, Department of Science and Technology, Linköping University, SE-60174 Norrköping, Sweden
[g] University of Helsinki, Department of Chemistry, P.O. Box 55 (A.I. Virtanens Plats 1), IN-00014 University of Helsinki, Finland
[h] Tomsk State University, 36 Lenin Avenue, Tomsk, Russia.
[i] College of Chemistry and Chemical Engineering, Henan University, Kaifeng 475004, China

ARTICLE INFO

Keywords:
Triplet fusion upconversion
Lanthanide
Nanocrystals
NIR dyes

ABSTRACT

Triplet fusion upconversion is useful for a broad spectrum of applications ranging from solar cells, photoredox catalysis, to biophotonics applications, especially in the near-infrared (NIR, >700 nm) range. This upconverting system typically demands efficient conversion of spin-singlet harvested energy through intersystem crossing to spin-triplet states, accessible only in rare metallic-coordinating macrocycle compounds or heavy-metal-containing semiconductor quantum dots for triplet sensitization. Herein, we describe an organic–inorganic system for NIR-to-visible triplet fusion upconversion, interfacing commonly-seen, non-metallic, infrared dyes (IR806, IR780, indyocynine green, and CarCl) and lanthanide nanocrystal (sodium ytterbium fluoride) as a hybrid molecular sensitizer, which extracts molecular spin-singlet energy to nanocrystal-enriched ytterbium dopants at ~48% efficiency (IR806, photoexciation at 808 nm). Moreover, ytterbium sub-lattice energy migration increases the interaction possibility between the nanocrystal and the freely-diffusing rubrenes in solution, resulting in 24-fold (IR806) to 1740-fold (indocyanine green) upconversion (600 nm) increase, depending on the IR dye type, as compared to the one without ytterbium nanotransducers. Ab initio quantum chemistry calculations identify enhanced spin-orbital coupling in the ytterbium-IR806 complex and high energy transfer rate in the ytterbium-rubrene interaction (10^{10} s^{-1}). Employing inorganic lanthanide nanocrystals as nanotransducers unleashes the potential use of non-metallic infrared organic dyes for triplet fusion upconversion.

1. Introduction

Optical upconversion that converts long-wavelength light to short-wavelength luminescence has gained increasing attention over the past decades [1,2]. Especially, near-infrared (NIR)-to-visible upconversion is of particular interest for finding applications in photoredox catalysis, deep-tissue bioimaging, optical super resolution imaging, volumetric displays, anti-counterfeiting, and solar cells [3–8]. Achieving NIR-to-visible upconversion can be realized through two-photon absorption (TPA) that necessitates simultaneous absorption of two photons, lanthanide upconversion that involves coupled linear excitation in ladder-like energy levels of trivalent lanthanide ions, and triplet fusion processes that utilize molecular pairs to store and fuse input energy at spin-triplet sates [9–11]. However, the optical nature of TPA and lanthanide upconversion demands high laser irradiance (>10^6 W/cm^2 for TPA; >10–100 W/cm^2 for lanthanide upconversion). This precludes their possibilities, with few exceptions on lanthanide upconversion, to upconvert incoherent light at low level of excitation irradiance [12,13]. Moreover, lanthanide ions have small (molar extinction coefficient, ~10^{-2} $M^{-1}cm^{-1}$) and narrow-band (~10 nm, full width of half maximum, FWHM) absorption, confining light harvesting abilities for upconversion. In contrast, triplet fusion upconversion (TFU) absorbs photons with molecular dyes (triplet sensitizers) that process large molar extinction coefficients (~10^3 $M^{-1}cm^{-1}$, five orders of magnitude higher than that

* Corresponding author at: School of Chemistry and Chemical Engineering, Harbin Institute of Technology, Harbin 150090, China.
E-mail address: chenguanying@hit.edu.cn (G. Chen).

https://doi.org/10.1016/j.cej.2021.131282
Received 10 April 2021; Received in revised form 5 June 2021; Accepted 3 July 2021
Available online 13 July 2021

of lanthanide ions) and in a broad spectral range (~100 nm, FWHM). This optical feature entails optical upconversion with photoexcitation at low-level light irradiance, even below sun irradiance (100 mW/cm^2) [14–16], creating numerous opportunities for sunlight-driven photochemical applications.

Enacting TFU requires molecular triplet sensitizers, typically, an organometallic compound (Fig. 1a), to absorb incident light and form an excited spin singlet state (S_1), which is then converted, through an intersystem crossing (ISC) process, to a dark spin-triplet state (T_1) for input energy store. Note that, recently, semiconductor quantum dots (Fig. 1b) have also been shown to be able to function as inorganic triplet molecular sensitizer due to the ease of spin relaxation of their excitons [17,18]. Energy is then transferred from the triplet state of the sensitizer to a triplet state of the annihilator (or acceptor). A pair of triplets on separate annihilator molecules can undergo a diffusion-mediated fusion process to form a single higher-energy singlet exciton for luminescence. Extensive studies have led to identify a set of sensitizer/annihilator molecular pairs for visible-to-visible and visible-to-ultraviolet upconversion (Excitation, 695–442 nm; Emission, 560–360 nm, depending on the molecular pair) [1]. Importantly, molecular engineering of organic triplet sensitizers and inorganic quantum dots enables a fine control over the intersystem crossing and/or triplet level positions, enriching production of triplet states that match the ones of the annihilator molecules [19,20]. As a result, ultrahigh upconversion quantum yields (UCQY ~30%; with a theoretical maximum of 100%) have been achieved for visible-to-visible triplet fusion upconversion as exemplified using 3,8-substituted Ir (III)-coordinated 1,10-phenanthroline molecular as triplet sensitizer and 9,10-diphenylanthracene (DPA) as annihilator (Excitation = 473, Emission = 430) [21]. In the meanwhile, heavy-metal-free organic sensitizers have also been developed as a proper alternative of low-cost and eco-friendly to noble or transition metal complexes. Some nonmetallic organic sensitizers, such as halogens dyes, "BODIPY" derivatives and TADF molecular variants have been applied to TFU successfully [22–24]. Despite recent progresses, limited success has been met in triplet fusion upconversion with incident wavelengths in the NIR range. This is because of the exponential increase in non-radiative losses in the molecular sensitizers with smaller energy gaps, which competes with the ISC and de-excites the triplet state, posing experimental challenge to create molecular sensitizers in the infrared. Indeed, only rare metallic-coordinating macrocycle compounds or heavy-metal-containing semiconductor quantum dots (PbS), with evidenced strong spin-orbital coupling, have been reported as molecular sensitizers for NIR triplet fusion upconversion [25–27].

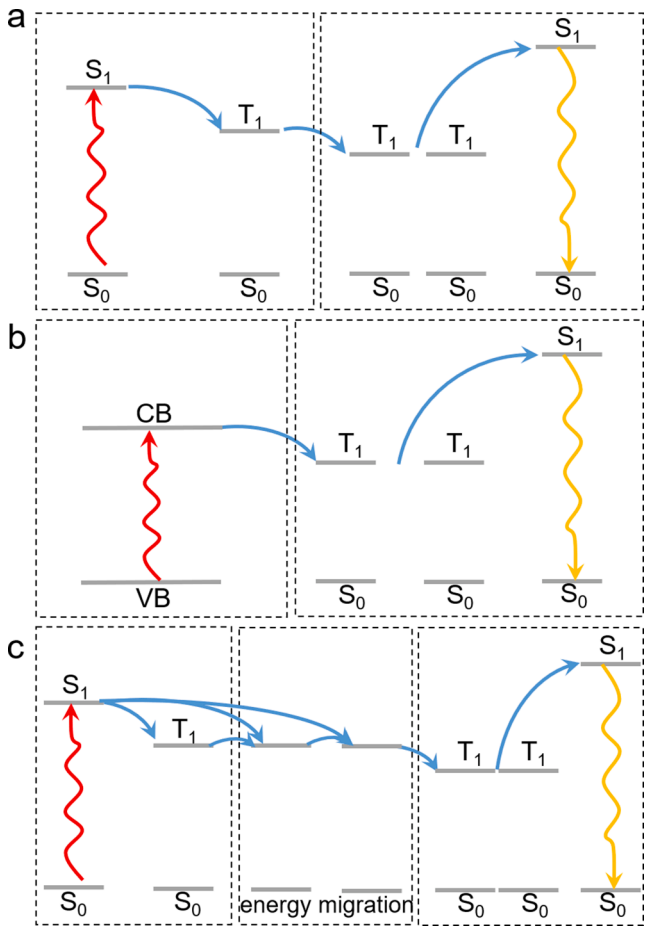

Fig. 1. Schematic illustration of triplet fusion upconversion mechanisms. (a) Triplet fusion upconversion via ISC (Intersystem Crossing) and TET (Triplet-to-Triplet Energy Transfer): the process is launched by the sensitizer absorbing excitation energy and triggering ISC to form an active triplet state (T_1). Subsequently, the energy is transferred to another T_1 state of a neighboring acceptor via TET. Two T_1 acceptor molecules are likely to collide and annihilate to form an S_1 state and emit upconversion fluorescence. (b) Inorganic semiconductor quantum dots as triplet sensitizer: the inorganic sensitizers absorbing excitation energy and transferring the energy to the T_1 state of the acceptor molecules. Two T_1 acceptor molecules are annihilated by collision, an S_1 and an S_0 state can be formed. (c) Triplet fusion upconversion via nanoparticle-mediated energy transfer to the annihilator, involving extraction of singlet and/or triplet energy across the organic/inorganic interface to the inorganic nanoparticles, energy migration among nanoparticles, and interfacial energy transfer to the triplet state of the acceptor for triplet fusion.

Though being unsuitable for triplet sensitization, the commonly-seen, non-metallic, infrared dyes possess similar high molar extinction coefficients and broad absorption spectra in the NIR region. Importantly, we notice that these non-metallic infrared dyes can be utilized not only as molecular antenna to sensitize lanthanide ions in doped nanocrystals to enhance the lanthanide luminescence [13,28], but also as molecular acceptors to quench lanthanide luminescence in doped nanocrystals through non-radiative energy transfer processes [29,30]. Very recently, triplet excitons were shown to be generated in lanthanide ion doped nanocrystals–organic molecule hybrid systems [31,32]. These facts illustrate the possibility to use lanthanide ions, with spin-relaxed energy states, as intermediary platforms to mediate the flow of input energy from the spin-singlet state of a molecular sensitizer to the spin-triplet state of the annihilator. This can avoid the necessitated use of a typical metallic-containing molecular triplet sensitizer with demanding spin-orbital coupling for triplet fusion upconversion.

Herein, we describe the conceptual use of inorganic nanocrystals (sodium ytterbium fluoride, $NaYbF_4$) as nanotransducers to activate the commonly seen nonmetallic infrared dyes, as exemplified here with the IR806 dye, for triplet fusion upconversion (Fig. 1c). Dye IR806 possesses a singlet state (S_1) at 1.54 eV (806 nm) and a triplet state (T_1) at 1.26 eV (980 nm) allowing absorption of photons in the NIR region [23,28]. A rigid conjugate organic molecular rubrene (PLQY ~100%), with T_1 at 1.14 eV (1090 nm), was utilized as the annihilator. Ytterbium (Yb^{3+}) dopants in the $NaYbF_4$ nanocrystals have two exclusive energy levels (the ground state $^2F_{2/7}$ and the excited sate $^2F_{2/5}$, with an energy space of 1.25 eV). An abundance of Yb^{3+} dopants in the lattice allows high-efficiency interfacial energy extraction (from surface NIR dye as energy donors), energy migration (among Yb^{3+}-sublattice), and lanthanide interaction with the annihilator (rubrene), thus channeling the input energy to the triplet states of rubrene for triplet fusion upconversion. Indeed, we show that attaching IR806 dye antenna to the surface of $NaYbF_4$ nanocrystals resulted in over 24-fold upconversion luminescence (600 nm) enhancement, as compared to the IR806-rubrene counterpart, along with an upconversion quantum yield (UCQY) increase from 0.6% to 1.38% (please refer to section 2.7 for the UCQY definition with a theoretical maximum of 100%) under photoexcitation at 808 nm. Meanwhile, an encapsulation of the hybrid IR806-nanocrystal-rubrene system in an oxygen-barrier poly(vinyl alcohol) (PVA) polymer enables stable NIR-to-visible triplet fusion upconversion

in a solid film for>12 h in air. Importantly, $NaYbF_4$ nanotransducers are demonstrated to be able to activate a set of other non-metallic infrared organic dyes (IR783, indyocynine green, and CarCl) for triplet fusion upconversion, resulting in about 19- to 1740-fold upconversion enhancement as compared to the control without the nanotransducers.

2. Experimental procedures

2.1. Chemicals and instrumentation

Chemical reagents were purchased from Sigma Aldrich, except that anhydrous *N,N'*-dimethylformamide (DMF), rubrene, and 4-mercaptobenzoic acid were purchased from Aladdin Industrial Inc. All chemicals were used as received. Anhydrous toluene and chloroform were prepared by redistilling and vacuuming and stored in the glove box.

The size and morphology of the nanoparticles was measured by the transmission electron microscope (TEM, Tecnai G2 Spirit Twin 12). The Powder X-ray diffraction (XRD) data was performed on a Rigaku D/max-γB diffractometer at the scanning rate of 1° min^{-1} in the 2θ range of 10 – 80°. Proton nuclear magnetic resonance (^1H NMR) spectra were recorded on a Bruker 400 using $CDCl_3$ as solvent at room temperature. Fourier transmission infrared (FTIR) spectra were collected on a Perkin Elmer Spectrum 100 spectrophotometer using KBr pellet disk in the range of 4000–500 cm^{-1}. Absorption spectra were recorded on an Agilent Cary5000 UV-Vis-NIR spectrophotometer in toluene in a quartz cuvette with a path length of 1 cm. The luminescence spectra and decay curves were collected by an Edinburgh FLS1000 spectrofluorometer equipped with an 808 nm and 980 nm diode laser (MLL-III-808/980-2W, Changchun New Industries Optoelectronics Tech Co.) that can operate in both continuous-wave and pulse mode, and equipped with a Xenon lamp. All dry and degassed samples were prepared in a MIKROUNA Ipure super purified glove box.

2.2. Synthesis of IR806 dye

IR806 was synthesized using the standard Schlenk technique and following a procedure reported previously with some modifications [33]. A mixture of IR780 iodide (250 mg, 0.375 mmol) and 4-meracptobenzoic acid (115 mg, 0.75 mmol) was dissolved in 10 mL of anhydrous DMF and stirred at room temperature overnight under N_2. The solution was filtered through a 0.45 μm PTFE syringe filter, followed by slowly adding diethyl ether to precipitate the product. The precipitate was collected by centrifugation, washed with diethyl ether, and dried under vacuum. NMR (500 MHz, CD_3OD): δ 8.54 (d, 2H), 7,92 (d, 2H), 7.36–7.63 (m, 10H), 6.36 (d, 2H), 4.14 (t, 4H), 2.71 (m, 4H), 1.94 (m, 2H), 1.79 (q, 4H), 1.17 (s, 13H), 0.92 (t, 6H).

2.3. Synthesis of $NaLnF_4$ nanocrystals (NCs).

Tiny $NaLnF_4$ (Ln = Yb, Y, Lu, Tm, Gd, Nd, Ce, and La) NCs was prepared following our previously reported method with adaptations [34]. First, an Ln-OA precursor was prepared using the following procedure. 1 mmol $LnCl_3{\cdot}6H_2O$ and 3 mmol sodium oleate were mixed with 3 mL deionized water, 3.5 mL absolute ethyl alcohol and 7 mL hexane, and the resulting mixture was heated at 60 °C overnight. The organic phase solvent containing Ln-OA was collected through a separatory funnel, and washed three times with deionized water in a separatory funnel. Second, the obtained Ln-OA precursor were mixed with 4 mmol sodium oleate, 5.2 mL OA, 5.1 mL OM and 9 mL ODE. The solution was then heated up to 100℃ under argon gas protection with vigorous magnetic stirring for 60 min. Subsequently, 4 mmol solid ammonium fluoride was added to the solution and kept at 100℃ for another 30 min. Last, the reaction mixture was heated to 300℃ at a rate of 10 $K{\cdot}min^{-1}$, and kept at this temperature for 30 min, then allowed to cool down to room temperature naturally. The resulting tiny $NaLnF_4$ was precipitated by addition of 20 mL ethanol, collected via centrifugation at 6000 rpm for 10 mins, washed twice with a 1:6 hexane/ethanol mixture, and finally dispersed in 10 mL hexane for further uses.

2.4. Preparation of IR806-rubrene mixed solution

IR806 (1.5 mg, 0.002 mmol) and rubrene (10 mg, 0.02 mmol) were added to a 1 mL anhydrous toluene. An ultrasonication was then applied to the mixture till the complete dissolvement of the solid dye powders. All the procedures were performed in an N_2 glove box.

2.5. Preparation of IR806-$NaLnF_4$-rubrene mixed solution

The as-prepared $NaLnF_4$ NCs are coated with the pristine ligand of oleic acid. To attach IR806 molecule to the $NaLnF_4$ (Ln = Yb, Y, Lu, Tm, Gd, Nd, Ce, and La) nanocrystal surface, a ligand exchange procedure was then implemented to substitute part of the surface oleic acid with IR806 dye molecule that contains the functional groups of carboxylate [3]. In a typical procedure, 1 mL of oleic acid-coated $NaLnF_4$ NCs in hexane (with a concentration of 0.1 mol/L) was centrifugated at 6000 rpm for 5 min, yielding a white pellet at the bottom of the centrifugation tube. Subsequently, the white pellet was placed into a glass vial, transferred into an N_2 glove box, and dissolved in 1 mL anhydrous $CHCl_3$. In a separate glass vial, 3 mg IR806 was dissolved in 1 mL anhydrous $CHCl_3$, which was then mixed with the NCs solution under magnetic stirring for 2 h at room temperature. The IR806- $NaLnF_4$ complex was precipitated from the mixed solution by adding excessive amount of acetone and collected via centrifugation at 6000 rpm for 5 min. The IR806-functionalized NCs pellet (green color) at the bottom of micro-centrifuge tube was then transferred into the N_2 glove box, resuspended in 1 mL anhydrous toluene, and mixed with 1 mL solution of rubrene (10 mg/mL). Lastly, the mixed IR806-$NaLnF_4$-rubrene mixed solution was stored in the glovebox for 24 h.

2.6. Estimations on the density of IR806 molecules on the surface of NCs.

The density of β-$NaYbF_4$ was 6.41×10^{-21} g/nm^3 [35], while the size of Yb-NCs that used in this work is ~11 nm, resulting in a total NC volume of 696 nm^3. As a consequence, the weight per single NC is calculated to be $696 \times 6.41 \times 10^{-21} = 4.46 \times 10^{-18}$ g, leading to a molar mass of $6.02 \times 10^{23} \times 4.46 \times 10^{-18} = 2.69 \times 10^6$ g/mol for the inorganic $NaYbF_4$ core ($MW_{core} = 2.69 \times 10^6$ g/mol).

In addition, the density of oleylamine molecules (MW = 267.5) on the surface of NCs was reported to be about 5/nm^2 [36], while a total NC surface area was calculated to be 379.94 nm^2 for a 11 nm-sized single NC. This leads to about ~1890 oleylamine molecules on one single NC surface, and thus a corresponding molar mass of 5.1×10^5 g/mol for the oleylamine shell per single NC.

As a consequence, the total molar mass (MW_{total}) of oleylamined-coated NCs was calculated to be $MW_{core} + MW_{oleylamine\ shell} = 3.2 \times 10^6$ g/mol. In the process of constructing the IR806-NCs-rubrene system, the optimum weight ratio for NCs:IR806 is 130 mg: 3 mg (43:1). According to the molar weight, we estimated the number of IR806 (MW = 784) on the surface of a single NC to be about 89, if all added dye molecules are attached to the surface of NCs. However, we identified that the absorbance of IR 806 molecules in IR806-NCs samples (after centrifugation to get rid of unattached IR 806 dyes) was ~54% of the one of IR806 molecule solution, indicating that 54% of added IR 806 molecules, *i.e.*, ~48 dye molecules, were attached to one single NCs surface.

2.7. Preparation of solid-sate upconversion film

IR806-rubrene film: IR806 (1.5 mg, 0.002 mmol) and rubrene (10 mg, 0.02 mmol) in THF (5 mL) was rapidly injected into 25 mL of 10 mM sodium dodecyl sulfate (SDS) aqueous solution. After 8 h of standing at 25 ℃, the precipitate was separated and purified by centrifugation at

10,000 rpm for 3 times. The precipitate was added to 15 wt% PVA/water solution. The suspension was casted on a glass plate and dried under vacuum.

IR806-NaYbF$_4$-rubrene film: The procedure to prepare the IR806-NaYbF$_4$-rubrene film is identical to that of the IR806-rubrene film, except that the IR806-NaYbF$_4$ complex was used to substitute IR806.

2.8. Measurement of upconverstion quantum yield

The upconversion quantum yield (Φ_{UC}) is calculated according to equation [37]:

$$\Phi_{UC} = 2\Phi_{std}\left(\frac{A_{std}}{A}\right)\left(\frac{I}{I_{std}}\right)\left(\frac{N}{N_{std}}\right)$$

where A_{std} and A are the numbers of photons absorbed by the standard reference sample (with known quantum yield) and the measured sample, respectively; I and I_{std} represent the integrated luminescence intensities of the measured sample and the standard reference sample, respectively; N and N_{std} are the average refractive index of the solvent used for dissolving the measured sample and the referenced standard sample, respectively. Here, indocynine green (ICG) dye in DMSO, with a known quantum yield of 12%, was utilized a standard reference to quantify Φ_{UC}. Note that a factor of 2 is introduced to the equation to reach a theoretical maximum of 100% [4,37]. This differs from another definition of UCQY in literature without the two-fold multiplication [38].

3. Results and discussion

Molecular IR806 dyes were synthesized using a simple one-step organic reaction between IR780 iodide and 4-mercaptobenzoic acid (Scheme S1), which meanwhile introduces a carboxylic group to the molecule that enables metallic coordination alongside the sulfate group. Observation of a broad absorption band (from 600 nm to 850 nm) peaked at 806 nm (Fig. 2a), in conjunction with a measured proton nuclear magnetic resonance (NMR) spectrum (Section 2.1), confirm the formation of the designated IR806 dye molecule. Mixing of IR806 and rubrene in anhydrous toluene in an N_2 environment resulted in the appearance of weak triplet fusion upconversion luminescence at 600 nm (photoexcitation, 808 nm), in marked contrast to null visible emission in the control samples of IR806-only or rubrene-only solution (Fig. 2b). An optimized concentration of 0.002 mol/L for IR806 and 0.02 mol/L for rubrene was identified for triplet fusion upconversion in toluene (Fig S1). The observed upconversion luminescence peak is consistent with the one of rubrene, except that the peak width was slightly narrowed due to photon reabsorption of rubrene at high concentrations (Fig. 2c). Measured excitation power density dependence of upconversion emission presents a slope = 2 below a threshold of 3.5 W/cm^2 and a slope = 1 above the threshold, which is characteristic of a triplet fusion upconversion process (Fig. 2e).

We examined the use of NaYbF$_4$ nanocrystals as nanotransducers to transfer the IR806-harvested energy to rubrene for enhanced triplet fusion upconversion. The NaYbF$_4$ nanocrystals were synthesized following an established procedure with adaptions, which adopt a hexagonal crystal phase (Fig. S2) and with a mean size of 11 nm (Fig. S3 and S4). Attaching IR806 to NaYbF$_4$ nanocrystals was achieved through a ligand exchange procedure, which enables substituting a fraction of the pristine oleic acid ligand on the nanocrystal surface with IR806. Observations of vibrational change in the spectral range of 1000–1750 cm^{-1} (Fig. S5) and optical absorption peak at 806 nm in IR806-NaYbF$_4$ (Fig. S6) are indicatives of a successful attachment to the nanocrystal surface. The acknowledgement of the attachment can also be supported by observing a strong dye antenna effect in IR806-NaYbF$_4$ (Fig. S7). Involving an optimized amount of NaYbF$_4$ nanocrystals (0.1 mol/L) in IR806-rubrene triplet fusion upconversion can lead to a 24-fold luminescence intensity increase (Fig. 2b and S9). This upconversion enhancement can also be clearly discerned from the photographic images of samples with and without NaYbF$_4$ nanocrystals (Fig. 2c). Moreover, the luminescence upconversion quantum yield (UCQY) of IR806-NaYbF$_4$-rubrene solution was determined to be 1.38% (maximal), about 2.3-fold higher than that of IR806-rubrene solution (Fig. S10). The slope of the power dependency of the emission intensity from quadratic (~2) to linear (~1) is a typical feature for the bimolecular TTA process.

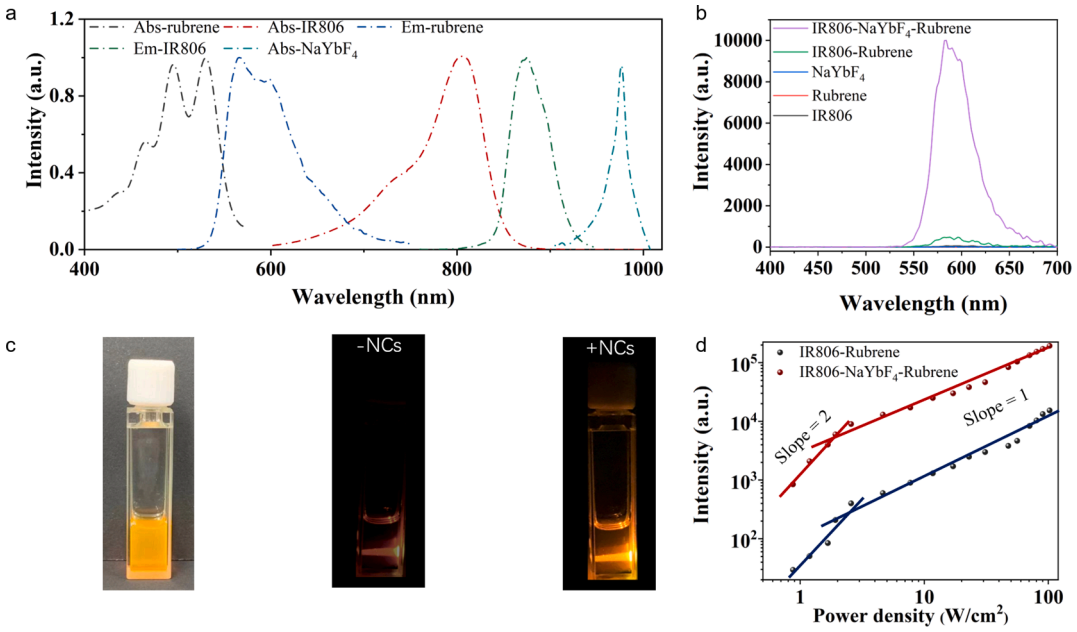

Fig. 2. Triplet fusion upconversion in IR806 sensitized rubrene and enhanced by NaYbF$_4$ nanocrystals. (a) Absorption and emission spectra of IR806 and rubrene in toluene. (b) Triplet fusion upconversion emission spectrum of IR806-rubrene and IR806-NaYbF$_4$-rubrene samples in toluene under photoexcitation at 808 nm (light irradiance, 1 W/cm^2). (c) Photographic images of IR806-NaYbF$_4$-rubrene solution taken under room lighting, as well as upconversion luminescence of IR806-rubrene (-NCs) and IR806-NaYbF$_4$-rubrene (+NCs) solutions taken in dark under photoexcitation at 808 nm (light irradiance, 1 W/cm^2); (d) Excitation power density dependence of upconversion emission intensities from IR806-rubrene and IR806-NaYbF$_4$-rubrene samples in toluene.

This clearly is a result of the competition between the TTA upconverting rate and the quenching rate (by surrounding centers) at the triplet state of the annihilator molecules. If the quenching rate is much higher than the TTA rate, the slope will be close to 2; oppositely, if the TTA rate is much higher than the quenching rate, the slope will be close to 1. Since higher power density leads to higher TTA rates, typically a slope change from 2 to 1 is observed in the TTA upconversion system [39–41]. The inflection threshold (for the slope = 2 to slope = 1 change) of IR806-$NaYbF_4$-rubrene was shifted to a power density of 2 W/cm^2, about 1.8-fold lower than that of the IR806 -rubrene (Fig. 2d). Higher UCQY and lower inflection power density indicate increased triplet fusion upconversion abilities for the IR806-$NaYbF_4$-rubrene.

Mechanistic investigations were performed to unveil the role of $NaYbF_4$ nanocrystals in triplet fusion upconversion in IR806-$NaYbF_4$-rubrene. We measured spin-singlet luminescence decay processes at 872 nm in free IR806 dyes (concentration 1.3 μM, toluene) and in IR806 dyes attached to the $NaYbF_4$ nanocrystal surface (concentration 1.3 μM, toluene) with an estimated amount of 10 dye molecules per nanocrystal (Fig. 3b). Attaching IR806 to the nanocrystal surface shortens the spin-singlet luminescence lifetime from 1.15 ns to 0.62 ns. This lifetime diminution corresponds to an extraction of about 46% of spin-singlet state energy across the organic/inorganic interface to nanocrystal Yb^{3+} dopants; this value is similar to the reported ones in IR806-sensitized $NaYF_4$:Yb^{3+}/Er^{3+} and $NaYF_4$:Yb^{3+}/Er^{3+}/Gd^{3+} (with enhanced ISC) lanthanide upconverting nanoparticles [23,26]. The spin-relaxed state of lanthanide ions (Yb^{3+}) allows energy channeling from the spin-singlet state of IR806 directly to Yb^{3+} dopants or from its spin-triplet state to Yb^{3+} dopants (Fig. 3a). The effective core potential (ECP) model with quasi relativistic simulation reveals that Yb^{3+} dopant increases the spin–orbit coupling matrix element (SOCME)$\langle S_1|H_{SO}|T_1\rangle$due to the heavy atom effect, resulting in an increased ISC rate of 2.3x10^9 s^{-1} that is higher than the one of 1.3x10^9 s^{-1} in iodine-containing IR806 dye (Supplementary Table S2). We also investigated the effect of a set of $NaLnF_4$ (Ln = Y, Lu, Tm, Gd, Ce, and La) nanocrystals on the triplet fusion upconversion (Fig. S11), presenting less than 2-fold upconversion enhancement as compared to the one in absence of the $NaLnF_4$ nanocrystals. This slight enhancement, produced by a set of atomic-distinct lanthanides, indicates that the contribution of the external heavy atom effect of Yb^{3+} to upconversion enhancement is less than 2-fold, in good agreement with the calculated ISC rate alteration. Direct excitation of Yb^{3+} dopants in $NaYbF_4$ nanocrystals at 980 nm resulted in the observation of triplet fusion upconversion luminescence of rubrene in $NaYbF_4$-rubrene and in IR806-$NaYbF_4$-rubrene solution, while no luminescence was observed in IR806-rubrene under identical photoexcitation conditions (Fig. 3c). This observation confirms that Yb^{3+} dopants in $NaYbF_4$ nanocrystals are able to sensitize the spin-triplet state of diffusing rubrene in solution. The observed stronger rubrene upconversion luminescence in $NaYbF_4$-rubrene than in IR806-$NaYbF_4$-rubrene is possibly ascribed to the existence of energy backflow from Yb^{3+} dopant at the $^2F_{5/2}$ state to the T_1 state of IR806. This is reasonable as the coupling between the $^2F_{5/2}$ state of Yb^{3+} and the T_1 state of IR806 is near-resonant (Fig. 3a, energy difference of ~52.2 cm^{-1}) [33]. We also used an optimized [rubrene-Yb]$^{3+}$ collision complex with a distance of 0.3 nm in between to calculate the energy transfer rate between the $^2F_{5/2}$ state of Yb^{3+} and the T_1 state of rubrene, which produces a considerable value of the $[D_i|H_{SO}|Q_1]$ SOCMEs that leads to an extremely fast transfer rate to 10^{10} s^{-1} between Yb^{3+} and rubrene (Supplementary Section 6). All these results indicate the important role of nanocrystal Yb^{3+} dopants-mediated energy transfers from the spin-singlet state of IR 806 to the spin-triplet state of rubrene for multiplied triplet fusion upconversion.

We also prepared a set of $NaYF_4$: Yb^{3+} x% (x = 10–100) nanocrystals to investigate the effect of Yb^{3+} dopant concentration on triplet fusion upconversion. Higher dopant concentrations clearly result in a monotonic luminescence increase in triplet fusion upconversion below 80%, while a near plateau was observed for Yb^{3+} dopant concentrations of 90–100%, giving direct evidence on the positive effect of the Yb^{3+} concentration on the number of emitted upconversion photons. When the concentration of Yb ions varying from 10% to 100%, the particle size increasing from 8.4 nm to 11.0 nm (Figs. S3 and S4), we can predict that the density of IR806 molecules is about 1/8 nm^2 per particle [28,33], so 27 to 48 dye molecules on the surface of single particle when the concentration of Yb ions is between 10% and 80%. As the doping concentration increases further, however, a slight size change results in a nearly constant number of dye molecules on the surface of the particles, so a nearly saturated upconversion enhancement is observed (Fig. 3d). We acquired time-resolved upconversion luminescence in IR806-rubrene and IR806-$NaYF_4$:Yb^{3+}-rubrene with varied Yb^{3+} dopant concentrations of 30%, 60%, and 100% (Fig. 3e). The increase of Yb^{3+} dopant concentration clearly elevates the upconversion luminescence rising time from 1.2 ± 0.20 μs in IR806-rubrene with null Yb^{3+} to 1.47 ± 0.22, 1.73 ± 0.02, and 1.94 ± 0.17 μs for Yb^{3+} dopant concentration of 30, 60 and 100%, respectively. Meanwhile, the upconversion luminescence decay process was also prolonged from 27.3 ± 0.4 μs at null Yb to 29.8 ± 1.1, 30.6 ± 1.8, and 36.9 ± 1.1 μs at Yb^{3+} dopant concentrations of 30, 60 and 100%, respectively. The Yb^{3+}-dependent increase of both rise and decay processes illustrates the excessive time required for the energy migration process in the Yb^{3+} sublattice of the nanocrystals. This energy migration process also escalates the interaction probabilities between surface Yb^{3+} dopants and diffusing rubrene for enhanced triplet fusion upconversion [42,43].

Triplet states generally suffer from significant quenching by moisture and molecular oxygen, dimming the triplet fusion upconversion in solution [44]. Moreover, the rubrene is prone to a cycloaddition reaction with singlet oxygen that deprives its role as triplet annihilator [45]. Nonetheless, the solar and detection applications require a solid-state architecture to produce air-stable upconversion. As a consequence, we implemented a simultaneous reprecipitation of rubrene and IR806 attached $NaYbF_4$ nanocrystals in tetrahydrofuran (THF) to produce hybrid microsized particles through a rapid injection into sodium dodecyl sulfate (SDS) aqueous solution. A suspension of these particles blended with polyvinyl alcohol (PVA)/water solution (15 wt%) can be deposited on a glass plate to produce a solid-state upconverting film (Fig. S12). Note that prolonging rise and decay times were observed in the solid-state thin film samples (Fig. S13), in analogy to the one in Fig. 3e, implying the same upconverting mechanism. We observed that $NaYbF_4$ nanocrystals result in 8-fold higher triplet fusion upconversion in the solid-state film as compared to the control film without $NaYbF_4$ nanocrystals. Note that the $NaYbF_4$-induced enhancement fold is about three times lower than the one (24-fold) in the solution system. This possibly suggests that about one third of the IR806-$NaYbF_4$ nanocomplexes remained intact during the reprecipitation process. Nevertheless, the solid-state upconversion luminescence remains constant over 12 h in air, which is analogous to the one for IR806-rubrene solution in N_2 environment, but in marked contrast to the IR806-rubrene solution in air (Fig. 4b). The stability of upconversion luminescence of the film in air is superior to the literature-reported ones (Supplementary Table S1). The 3D-printed mouse painted with IR806-rubrene film or IR806-$NaYbF_4$-rubrene film can emit precisely space-defined triplet fusion upconversion, presenting similar upconversion behavior as in the solid-state film. Importantly, besides the IR806 dye, $NaYbF_4$ nanotransducers are able to activate a set of the commonly-seen, non-metallic, infrared dyes for triplet fusion upconversion, multiplying rubrene upconversion by 899-fold, 1740-fold, and 19-fold for IR783, indocynine green (ICG), and CarCl dye molecules, respectively (Fig. 4d).

4. Conclusions

To conclude, we have described the conceptual use of $NaYbF_4$ nanocrystals as a nanotransducer to channel spin-singlet harvested photonic energy of the commonly-seen, non-metallic, infrared dyes (IR806) to the triplet state of diffusing rubrene (annihilator or acceptor) for NIR-to-visible triplet fusion upconversion. Interfacing the organic

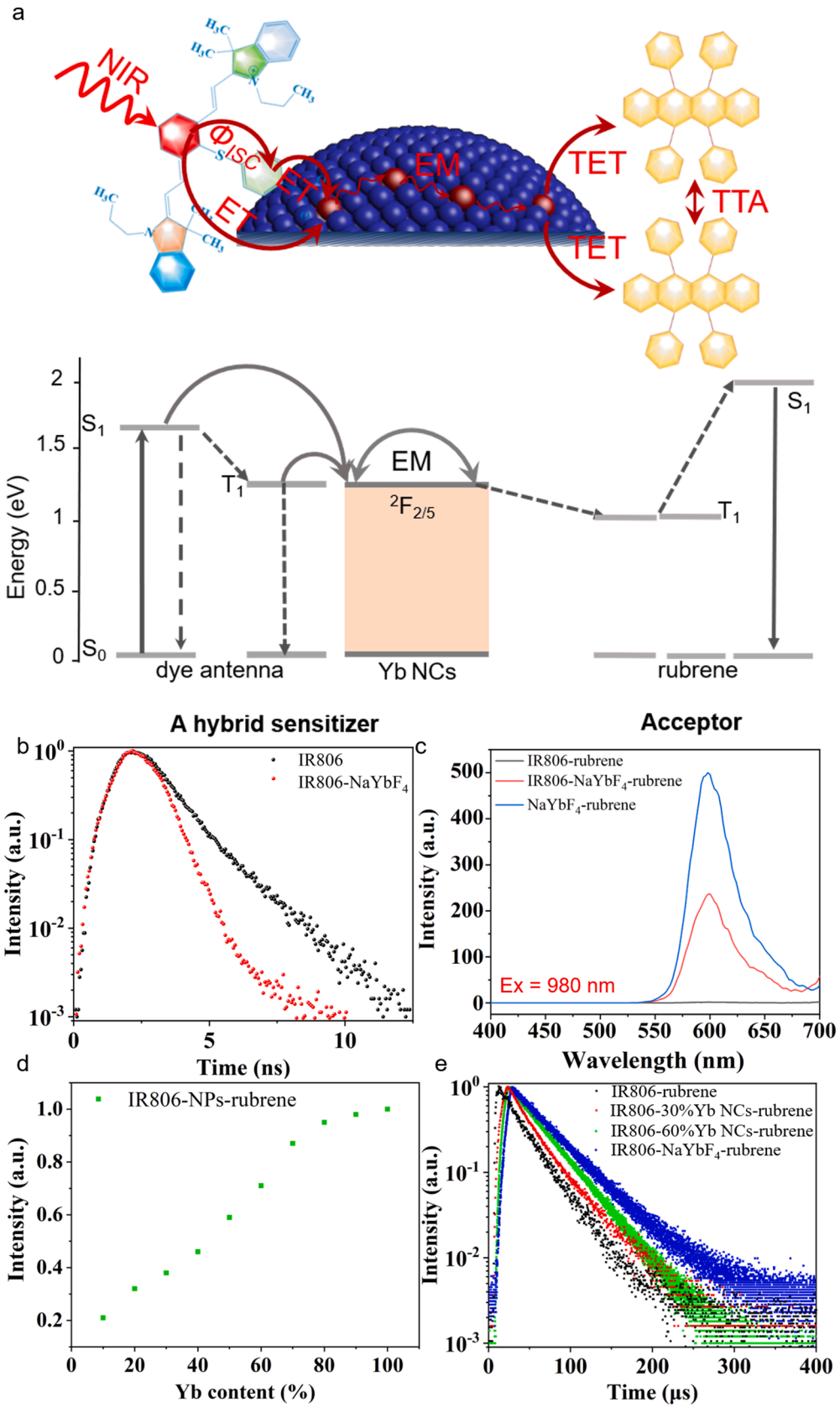

Fig. 3. Mechanistic investigation of triplet fusion upconversion involving $NaYbF_4$ nanocrystals. (a) A schematic illustration of involved energy transfer processes in the IR806-$NaYbF_4$-rubrene, whereby IR806 antenna interfaces $NaYbF_4$ nanocrystals forming a hybrid molecular sensitizer. Dye antenna on the nanocrystal surface absorbs the NIR incident light being excited to the spin-singlet state, from which energy can be transferred across the organic/inorganic interface to adjacent Yb^{3+} dopants in the nanocrystal or via ISC to the spin-triplet state that then resonantly sensitize the Yb^{3+} dopants. Energy migration withiin the Yb^{3+} sub-lattice provides high probabilities of surface Yb^{3+} dopants to interact with the spin-triplet state of rubrene, initializing triplet–triplet annihilation processes for upconversion. This is in marked contrast to the mechanism in IR806-rubrene, which relies on the sole ISC process, depending on the magnitude of molecular spin-orbital coupling, to produce spin-triplet states of IR806 that sensitize the spin-triplet states of rubrene through molecular collision in solution. (b) Decay lifetimes of the spin-singlet state of IR806 in the freely-diffusing form (black, 1.15 ns) and in the IR806-$NaYbF_4$ (red, 0.62 ns) complex, where IR806 is attached to the $NaYbF_4$ nanocrystal surface. (c) Emission spectra of IR806-rubrene, IR806-$NaYbF_4$-rubrene, and $NaYbF_4$-rubrene samples under photoexcitation at 980 nm (120 W/cm^2) which matches the absorption of the Yb^{3+} dopants. (d) Triplet fusion upconversion emission intensities utilizing $NaYF_4$:x%Yb^{3+} nanocrystals with varied amount of Yb^{3+} dopant concentrations (x = 10–100%). (e) Time-resolved luminescence decay of the upconversion emission (600 nm) from rubrene with increased dopant contents of Yb^{3+} in $NaYF_4$ nanocrystals under photoexciation at ~808 nm. (For interpretation of the references to color in this figure legend, the reader is referred to the web version of this article.)

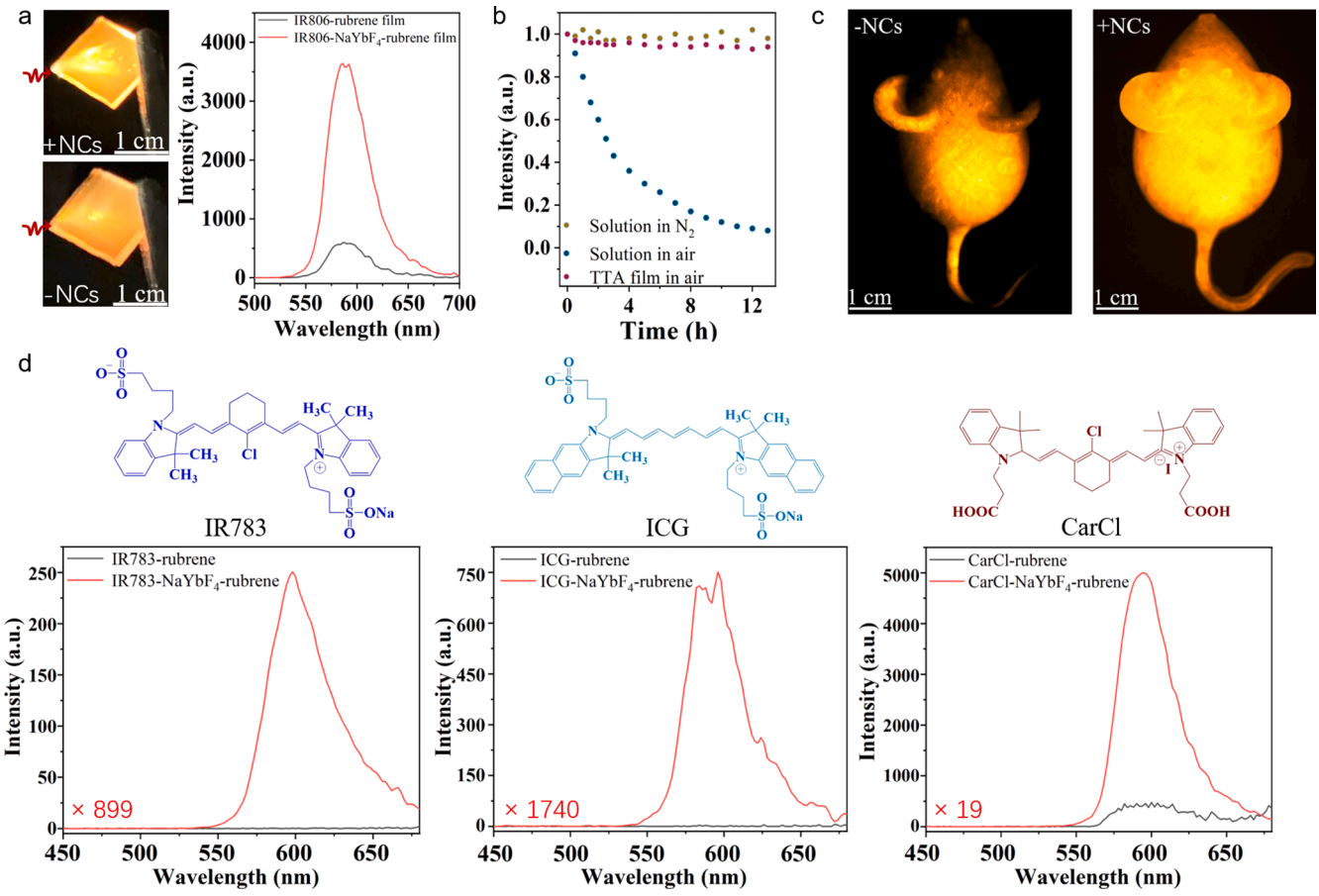

Fig. 4. Air-stable solid-film upconversion and activating non-metallic NIR dyes for triplet fusion upconversion through $NaYbF_4$ nanotransducers. (a) Photographic images (left) and emission spectra of triplet fusion upconversion in the IR806-rubrene and IR806-$NaYbF_4$-rubrene films (photoexcitation at 808 nm). (b) Emission stabilities of upconversion in IR806-rubrene solution in air and in N_2 environment, as well as in IR806-$NaYbF_4$-rubrene film in air. (c) Triplet fusion upconversion in 3D-printed mouse (polylactic acid (PLA) material) painted with IR806-rubrene film (left) and IR806-$NaYbF_4$-rubrene film (right). (d) Activation of dark IR783, indocyanine green (ICG), and CarCl NIR dye molecules to sensitize rubrene for triplet fusion upconversion (toluene solution) through interfacing $NaYbF_4$ nanocrystals. (For interpretation of the references to color in this figure legend, the reader is referred to the web version of this article.)

infrared dye with the inorganic nanocrystal forms a hybrid molecular sensitizer, in which the spin-singlet energy of the infrared dyes attached to the nanocrystal surface can be extracted to Yb^{3+} dopants in the nanocrystal at a high efficiency (~48%). Mechanistic investigations reveal that Yb^{3+} sublattice energy migration increases the probabilities to interact with freely-diffusing rubrene (annihilator) in solution, enabling a direct sensitization of the rubrene triplet state for enhanced triplet fusion upconversion. Indeed, the $NaYbF_4$ nanotransducers results in about 19- to 1740-fold upconversion (600 nm) increase in a set of non-metallic infrared molecular dyes (IR806, IR783, ICG, and CarCl), depending on dye type, as compared to the one without ytterbium nanotransducers. We believe that the described concept here bypasses the necessity of strong spin-orbital coupling for efficient spin-singlet to spin-triplet intersystem conversion in molecular sensitizers, thus untapping the potential use of the commonly-seen, non-metallic, NIR organic dyes for triplet fusion upconversion.

Declaration of Competing Interest

The authors declare that they have no known competing financial interests or personal relationships that could have appeared to influence the work reported in this paper

Acknowledgments

This work is supported by the National Natural Science Foundation of China (51972084 and 51672061), the State Key Laboratory of Urban Water Resource and Environment (Harbin Institute of Technology) (No. 2020DX10), and the Fundamental Research Funds for the Central Universities, China (AUGA5710052614). We thank Dr Xin Li, at the Royal Institute of Technology, Stockholm, Sweden, for inspirational discussions and for computations of the triplet fusion upconversion phenomenon. G. B. thanks for support to Swedish Research Council (grant No. 2020-04600). The computations were enabled by resources provided by the Swedish National Infrastructure for Computing (SNIC 2020-3-29) at the High Performance Computing Center North (HPC2N) partially funded by the Swedish Research Council through grant agreement no. 2018–05973. R. R. V. thanks for support to the Academy of Finland (grant number 1325369 and 1315600). The creation of energy transfer theoretical model and its implementation, including the ab initio quantum chemical calculations were done within the grant from the Russian Science Foundation (project No. 17-73-20012).

Appendix A. Supplementary data

Supplementary data to this article can be found online at https://doi.org/10.1016/j.cej.2021.131282.

References

[1] T.N. Singh-Rachford, F.N. Castellano, Photon upconversion based on sensitized triplet–triplet annihilation, Coor. Chem. Rev. 254 (2010) 2560–2573.

[2] K. Borjesson, P. Rudquist, V. Gray, K. Moth-Poulsen, Photon upconversion with directed emission, Nat. Commun. 7 (2016) 12689.

[3] M. Mahboub, P. Xia, J. Van Baren, X. Li, C.H. Lui, M.L. Tang, Midgap states in PbS quantum dots induced by Cd and Zn enhance photon upconversion, ACS Energy Lett. 3 (2018) 767–772.

[4] L. Nienhaus, J.P. Correa-Baena, S. Wieghold, M. Einzinger, T.A. Lin, K. E. Shulenberger, N.D. Klein, M. Wu, V. Bulović, T. Buonassisi, M.A. Baldo, M. G. Bawendi, Triplet-sensitization by lead halide perovskite thin films for near-infrared-to-visible up-conversion, ACS Energy Lett. 4 (2019) 888–895.

[5] D. Di, L. Yang, J.M. Richter, L. Meraldi, R.M. Altamimi, A.Y. Alyamani, D. Credgington, K.P. Musselman, J.L. MacManus-Driscoll, R.H. Friend, Efficient triplet exciton fusion in molecularly doped polymer light-emitting diodes, Adv. Mater. 29 (2017) 1605987.

[6] L. Huang, E. Kakadiaris, T. Vaneckova, K. Huang, M. Vaculovicova, G. Han, Designing next generation of photon upconversion: Recent advances in organic triplet-triplet annihilation upconversion nanopar-ticles, Biomaterials 201 (2019) 77–86.

[7] J. Park, M. Xu, F. Li, H.C. Zhou, 3D long-range triplet migration in a water-stable metal-organic framework for upconversion-based ultralow-power in vivo imaging, J. Am. Chem. Soc. 140 (2018) 5493–5499.

[8] Q. Liu, T. Yang, W. Feng, F. Li, Blue-emissive upconversion nanoparticles for low-power-excited bioimaging in vivo, J. Am. Chem. Soc. 134 (2012) 5390–5397.

[9] L. Sun, W. Zhu, W. Wang, F. Yang, C. Zhang, S. Wang, X. Zhang, R. Li, H. Dong, W. Hu, Intermolecular charge-transfer interactions facilitate two-photon absorption in styrylpyridine-tetracyanobenzene cocrystals, Angew. Chem. Int. Ed. 56 (27) (2017) 7831–7835.

[10] Y. Gu, Z. Guo, W. Yuan, M. Kong, Y. Liu, Y. Liu, Y. Gao, W. Feng, F. Wang, J. Zhou, D. Jin, F. Li, High-sensitivity imaging of time-domain near-infrared light transducer, Nat. Photon. 13 (2019) 525–531.

[11] Y. Han, S. He, X. Luo, Y. Li, Z. Chen, W. Kang, X. Wang, K. Wu, Triplet sensitization by "self-trapped" excitons of nontoxic $cuins_2$ nanocrystals for efficient photon upconversion, J. Am. Chem. Soc. 141 (2019) 13033–13037.

[12] Y. Zhong, I. Rostami, Z. Wang, H. Dai, Z. Hu, Energy migration engineering of bright rare-earth upconversion nanoparticles for excitation by light-emitting diodes, Adv. Mater. 27 (2015) 6418–6422.

[13] G. Chen, J. Damasco, H. Qiu, W. Shao, T.Y. Ohulchanskyy, R.R. Valiev, X. Wu, G. Han, Y. Wang, C. Yang, H. Agren, P.N. Prasad, Energy-cascaded upconversion in an organic dye-sensitized core/shell fluoride nanocrystal, Nano Lett. 15 (2015) 7400–7407.

[14] C. Fan, L. Wei, T. Niu, M. Rao, G. Cheng, J.J. Chruma, W. Wu, C. Yang, Efficient triplet-triplet annihilation upconversion with an anti-stokes shift of 1.08 ev achieved by chemically tuning sensitizers, J. Am. Chem. Soc. 141 (2019) 15070–15077.

[15] Y. Liu, K. Chen, S. Yang, D. Zheng, G. Ren, Y. Yang, J. Zhao, D. Wei, K. Han, Hetero-bichromophore dyad as a highly efficient triplet acceptor for polarity tuned triplet-triplet annihilation upconversion, J. Phys. Chem. Lett. 10 (2019) 4368–4373.

[16] H. Liu, X. Yan, L. Shen, Z. Tang, S. Liu, X. Li, Color-tunable upconversion emission from a twisted intramolecular charge-transfer state of anthracene dimers via triplet–triplet annihilation, Mater. Horiz. 6 (2019) 990–995.

[17] C. Mongin, S. Garakyaraghi, N. Razgoniaeva, M. Zamkov, F. Castellano, Direct observation of triplet energy transfer from semiconductor nanocrystals, Science 351 (2016) 369–372.

[18] Z. Huang, X. Li, M. Mahboub, K. Hanson, V. Nichols, H. Le, M. Tang, C. Bardeen, Hybrid molecule-nanocrystal photon upconversion across the visible and near-infrared, Nano Lett. 15 (2015) 5552–5557.

[19] J. Zhao, W. Wu, J. Sun, S. Guo, Triplet photosensitizers: from molecular design to applications, Chem. Soc. Rev. 42 (2013) 5323–5351.

[20] Z. Huang, Z. Xu, T. Huang, V. Gray, K. Moth-Poulsen, T. Lian, M.L. Tang, Evolution from tunneling to hopping mediated triplet energy transfer from quantum dots to molecules, J. Am. Chem. Soc. 142 (2020) 17581–17588.

[21] Y. Lu, J. Wang, N. McGoldrick, X. Cui, J. Zhao, C. Caverly, B. Twamley, G. Máille, B. Irwin, R. Conway-Kenny, S. Draper, Iridium(III) Complexes bearing pyrene-functionalized 1,10-phenanthroline ligands as highly efficient sensitizers for triplet-triplet annihilation upconversion, Angew. Chem. Int. Ed. 55 (2016) 14688–14692.

[22] W. Wu, H. Guo, W. Wu, S. Ji, J. Zhao, Organic triplet sensitizer library derived from a single chromophore (bodipy) with long-lived triplet excited state for triplet-triplet annihilation based upconversion, J. Org. Chem. 76 (2011) 7056–7064.

[23] S. Pristash, K. Corp, E. Rabe, C. Schlenker, Heavy-atom-free red-to-yellow photon upconversion in a thiosquaraine composite, ACS Appl. Energy Mater. 3 (2020) 19–28.

[24] A. Niwa, S. Haseyama, T. Kobayashi, T. Nagase, K. Goushi, C. Adachi, H. Naito, Triplet-triplet annihilation in a thermally activated delayed fluorescence emitter lightly doped in a host, Appl. Phys. Lett. 113 (2018), 083301.

[25] Y. Sasaki, M. Oshikawa, P. Bharmoria, H. Kouno, A. Hayashi-Takagi, M. Sato, I. Ajioka, N. Yanai, N. Kimizuka, Near-infrared optogenetic genome engineering based on photon-upconversion hydrogels, Angew. Chem. Int. Ed. 58 (49) (2019) 17827–17833.

[26] B.D. Ravetz, A.B. Pun, E.M. Churchill, D.N. Congreve, T. Rovis, L.M. Campos, Photoredox catalysis using infrared light via triplet fusion upconversion, Nature 565 (2019) 343–346.

[27] A.B. Pun, L.M. Campos, D.N. Congreve, Tunable emission from triplet fusion upconversion in diketopyrrolopyrroles, J. Am. Chem. Soc. 141 (2019) 3777–3781.

[28] W. Zou, C. Visser, J.A. Maduro, M.S. Pshenichnikov, J.C. Hummelen, Broadband dye-sensitized upconversion of near-infrared light, Nat. Photon. 6 (2012) 560–564.

[29] M. Kong, Y. Gu, Y. Liu, Y. Shi, N. Wu, W. Feng, F. Li, Luminescence lifetime-based in vivo detection with responsive rare earth-dye nanocomposite, Small 15 (46) (2019) 1904487.

[30] M. Zhao, B. Li, Y. Wu, H. He, X. Zhu, H. Zhang, C. Dou, L. Feng, Y. Fan, F. Zhang, A tumor-microenvironment-responsive lanthanide-cyanine fret sensor for nir-ii luminescence-lifetime in situ imaging of hepatocellular carcinoma, Adv. Mater. 32 (2020) 2001172.

[31] S. Han, R. Deng, Q. Gu, L. Ni, U. Huynh, J. Zhang, Z. Yi, B. Zhao, H. Tamura, A. Pershin, H. Xu, Z. Huang, S. Ahmad, M. Abdi-Jalebi, A. Sadhanala, M.L. Tang, A. Bakulin, D. Beljonne, X. Liu, A. Rao, Lanthanide-doped inorganic nanoparticles turn molecular triplet excitons bright, Nature 587 (2020) 594–599.

[32] B. Zheng, D. Zhong, T. Xie, J. Zhou, W. Li, A. Ilyas, Y. Lu, M. Zhou, R. Deng, Near-infrared photosensitization via direct triplet energy transfer from lanthanide nanoparticles, Chem 7 (2021) 1615–1625.

[33] D.J. Garfield, N.J. Borys, S.M. Hamed, N.A. Torquato, C.A. Tajon, B. Tian, B. Shevitski, E.S. Barnard, Y.D. Suh, S. Aloni, J.B. Neaton, E.M. Chan, B.E. Cohen, P.J. Schuck, Enrichment of molecular antenna triplets amplifies upconverting nanoparticle emission, Nat. Photon. 12 (2018) 402–407.

[34] H. Li, L. Xu, G. Chen, Controlled synthesis of monodisperse hexagonal $nayf_4$:yb/er nanocrystals with ultrasmall size and enhanced upconversion luminescence, Molecules 22 (2017) 2113.

[35] Y. Pyatenko, A. Voronkov, The formula of fagarinite, J. Struct. Chem. 3 (1962) 696–697.

[36] A. Ulman, Formation and structure of self-assembled monolayers, Chem. Rev. 96 (1996) 1533–1554.

[37] L. Huang, W. Wu, Y. Li, K. Huang, L. Zeng, W. Lin, G. Han, Highly effective near-infrared activating triplet triplet annihilation upconversion for photoredox catalysis, J. Am. Chem. Soc. 142 (2020) 18460–18470.

[38] V. Gray, D. Dzebo, M. Abrahamsson, B. Albinsson, K. Moth-Poulsen, Triplet-triplet annihilation photon-upconversion: towards solar energy applications, PCCP 16 (22) (2014) 10345–10352.

[39] A. Monguzzi, J. Mezyk, F. Scotognella, R. Tubino, F. Meinardi, Upconversion-induced fluorescence in multicomponent systems: steady-state excitation power threshold, Phys. Rev. B. 78 (2008), 195112.

[40] Y. Cheng, B. Fuckel, T. Khoury, R. Clady, M. Tayebjee, N. Ekins-Daukes, M. Crossley, T. Schmidt, Kinetic analysis of photochemical upconversion by triplet-triplet annihilation: beyond any spin statistical limit, J. Phys. Chem. Lett. 1 (2010) 1795–1799.

[41] A. Haefele, J. Blumhoff, R. Khnayzer, F. Castellano, Getting to the (square) root of the problem: how to make noncoherent pumped upconversion linear, J. Phys. Chem. Lett. 3 (2012) 299–303.

[42] M. Wu, D.N. Congreve, M.W.B. Wilson, J. Jean, N. Geva, M. Welborn, T. Van Voorhis, V. Bulović, M.G. Bawendi, M.A. Baldo, Solid-state infrared-to-visible upconversion sensitized by colloidal nanocrystals, Nat. Photon. 10 (2015) 31–34.

[43] P. Bharmoria, S. Hisamitsu, H. Nagatomi, T. Ogawa, M.A. Morikawa, N. Yanai, N. Kimizuka, Simple and versatile platform for air-tolerant photon upconverting hydrogels by biopolymer-surfactant-chromophore co-assembly, J. Am. Chem. Soc. 140 (2018) 10848–10855.

[44] S.H.C. Askes, S. Bonnet, Solving the oxygen sensitivity of sensitized photon upconversion in life science applications, Nat. Rev. Chem. 2 (2018) 437–452.

[45] D.D. Mastrogiovanni, J. Mayer, A.S. Wan, A. Vishnyakov, A.V. Neimark, V. Podzorov, L.C. Feldman, E. Garfunkel, Oxygen incorporation in rubrene single crystals, Sci. Rep. 4 (2014) 4753–4758.